Atmospheric Environment 358 (2025) 121352

Contents lists available at ScienceDirect

Atmospheric Environment

journal homepage: www.elsevier.com/locate/atmosenv

The impact of biomass burning emissions in Southeast Asia on black carbon aerosols in southern China

Luhang Liu [a], Yu-Hao Mao [a,b,*], Hong Liao [a,b]

[a] Jiangsu Key Laboratory of Atmospheric Environment Monitoring and Pollution Control/Jiangsu Collaborative Innovation Center of Atmospheric Environment and Equipment Technology, School of Environmental Science and Engineering, Nanjing University of Information Science and Technology (NUIST), Nanjing, 210044, China
[b] Key Laboratory of Meteorological Disaster, Ministry of Education (KLME)/Collaborative Innovation Center on Forecast and Evaluation of Meteorological Disasters (CIC-FEMD)/International Joint Research Laboratory on Climate and Environment Change (ILCEC), NUIST, Nanjing, 210044, China

HIGHLIGHTS

- BBSEA contribute 2 %–73 % of BC concentrations in southern China (SC) in spring 2014.
- Contributions of BBSEA to BC in SC increase by 4 %–14 % in March 2019 compared to 2014.
- Transport time of BBSEA to Guangzhou is 2–6 days at 700 hPa in March 2014.

GRAPHICAL ABSTRACT

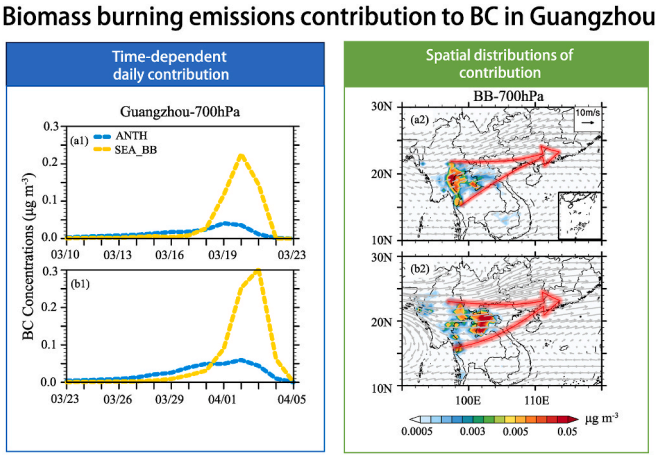

ARTICLE INFO

Keywords:
Black carbon
Biomass burning emissions
Southeast asia
Source attribution
Adjoint simulation

ABSTRACT

Since 2013, China's air quality has significantly improved due to the reduction of anthropogenic emissions. The influence of long-distance transport of biomass burning emissions in Southeast Asia (BBSEA) on air quality in southern China (SC) would likely continue to increase, especially under the trend of global warming. We quantify the contribution of BBSEA to the surface and high-altitude BC concentrations in SC (two provincial capitals: Guangzhou (GZ), Guangdong, and Kunming (KM), Yunnan) in March–April 2014 and 2019 by using the GEOS-Chem global chemical transport model and its adjoint. For three severe pollution events in SC in 2014, the contributions of BBSEA to daily average BC concentrations in GZ are 0.08–0.19 μg m^{-3} (2 %–5 %) at the surface and 0.20–0.78 μg m^{-3} (59 %–73 %) at 700 hPa. In KM, the corresponding contributions are 0.27–0.54 μg m^{-3} (15 %–33 %) and 0.25–0.45 μg m^{-3} (28 %–45 %). The transport time of BBSEA to the surface of GZ (KM) is about

This article is part of a special issue entitled: Atmospheric black carbon published in Atmospheric Environment.

* Corresponding author. School of Environmental Science and Engineering, Nanjing University of Information Science and Technology (NUIST), Nanjing, 210044, China.
E-mail address: yhmao@nuist.edu.cn (Y.-H. Mao).

https://doi.org/10.1016/j.atmosenv.2025.121352
Received 11 April 2025; Received in revised form 27 May 2025; Accepted 10 June 2025
Available online 12 June 2025

3–6 days (1–5 days). The shift in wind fields from southwest to west and stronger wind speeds in April likely shorten the transport time of BBSEA to SC. On March 27, 2019, the relative contributions of BBSEA to the surface BC concentrations increase by 10 % in GZ and 14 % in KM, compared to March 23, 2014. Our study would offer scientific support for understanding BC sources and potential improvement of air quality in SC.

1. Introduction

Black carbon (BC), as an important $PM_{2.5}$ component, is mainly produced by the incomplete combustion of fossil fuel, biofuel, and biomass burning emissions (Lin et al., 2025; Pauraite et al., 2021; Zong et al., 2016). BC influences the Earth's radiation budget directly by absorbing radiation and indirectly by changing the cloud formation (Chan, 2017; Zhuang et al., 2025). BC also accelerates the melting of glaciers and snow by reducing surface albedo, affecting global climate (Li et al., 2019; Zhang et al., 2025). BC has unique structural properties that adsorb toxic pollutants and causes serious harm to the human respiratory tract and cardiovascular systems (Nam et al., 2008; Rasking et al., 2023; Roy et al., 2024). In addition, BC has a small particle size and relatively long residence time in the atmosphere, so it can be transported to areas thousands of kilometers away from the source, affecting the air quality along the way (Hu et al., 2022; Li et al., 2021; Menegoz et al., 2011).

Since 2013, China has issued the Action Plan for the Prevention and Control of Air Pollution (https://www.gov.cn/zwgk/2013-09/12/content_2486773.htm, last access: April 2, 2025), the Three-Year Action Plan for Winning the Blue Sky Defense Battle (https://www.gov.cn/zhengce/content/2018-07/03/content_5303158.htm, last access: April 2, 2025), and the Action Plan for Continuous Improvement of Air Quality (https://www.gov.cn/zhengce/content/202312/content_6919000.htm, last access: April 2, 2025), the quality of China's atmospheric environment has been greatly improved. As a result of these initiatives, the annual average $PM_{2.5}$ concentrations in southern China (Yunnan, Guangxi, and Guangdong Provinces), are generally below the Grade II of the Chinese Ambient Air Quality Standard (CAAQS, 35 μg m^{-3}) (Wei et al., 2024). Guangzhou is the capital of Guangdong Province, the observed annual average $PM_{2.5}$ concentrations declined to approximately 19.56 μg m^{-3} in 2022 (Geng et al., 2024), and the annual average BC concentrations dropped from 3.35 μg m^{-3} in 2013 to 1.59 μg m^{-3} in 2018 (Lin et al., 2019; Pei et al., 2023). The annual average $PM_{2.5}$ concentrations in Yunnan Province have also decreased from 39.28 μg m^{-3} in 2013 to 23.92 μg m^{-3} in 2021 (Li et al., 2023). Previous studies have shown that $PM_{2.5}$ concentrations in southern China are influenced by local emissions and also atmospheric transport, particularly from Southeast Asia, and the contributions of biomass burning emissions from Southeast Asia (BBSEA) to $PM_{2.5}$ concentrations at high altitude in southern China can reach up to 20 %–70 % (Fu et al., 2012; Li et al., 2022; Zhang et al., 2016). As local anthropogenic emissions in southern China continue to decline, the contributions of atmospheric transport of BBSEA to southern China will become increasingly prominent, particularly under the trend of global warming, which would hinder further improvements in air quality in the southern China.

Biomass burning emissions are significant sources of environmental pollution, and have important impacts on air quality, climate change, and human health by emitting gases and particulate matters into the troposphere, which thus have garnered substantial attention over the past few decades (Andreae, 2019; Randerson et al., 2017; Yin et al., 2019). Additionally, pollutants emitted from biomass burning can be transported over long distances, frequently resulting in severe air pollution in areas situated downwind of the source (Fu and Jian, 2014; Wang et al., 2009). Southeast Asia is one of the most intensive regions for biomass burning emissions in the world, which contributes to around 5 percent of global biomass burning emissions, but covers only about 1 percent of the world's land area (Randerson et al., 2017). Emissions from biomass burning in southeast Asia are likely to increase in the future under the influence of global warming (Liu et al., 2024; Yin, 2020). For example, Zhang et al. (2024) predicted that the burned area in Southeast Asia will increase by about 0.0012 Mha (~30 %) under the shared socioeconomic pathways (SSP126) scenario during 2021–2040 compared to the reference period (1997–2021). There is a distinct seasonal variation in BBSEA, and approximately 69 %–82 % of the annual emissions are emitted from February to April and 50 % in March (Chan, 2017; Lin et al., 2009; Yang et al., 2022; Yin et al., 2019).

Southern China is situated close to Southeast Asia, and the pollutants from BBSEA significantly impact air quality in southern China by strong westerly winds, especially in March and April (Liu et al., 2023; Yang et al., 2022; Zhang et al., 2022). The Yunnan Province, which borders Southeast Asia, is most severely affected by BBSEA. Yang et al. (2022) demonstrated that BBSEA accounted for 69 % of the surface average $PM_{2.5}$ concentrations in Yunnan Province during the heavy pollution period in 2017 by using the Weather Research and Forecasting model coupled with Chemistry (WRF-Chem). Li et al. (2024) employed the Regional Air Quality Model System (RAQMS) to show that BBSEA contributed over 50 % of total tropospheric $PM_{2.5}$ concentrations in southern China in March 2008–2019. Liu et al. (2023) adopted the Hybrid Single-Particle Lagrangian Integrated Trajectory (HYSPLIT) model to show that the contribution of BBSEA to the surface average BC concentrations in Xishuangbanna in Yunnan Province was 77 % in March–April 2017. In addition, Guangzhou in Guangdong Province is situated downwind of the Southeast Asia spring monsoon and is also affected by the long-range transport of pollutants emitted from BBSEA (Huang et al., 2023; Zhu et al., 2011, 2024). The aerosol optical depth (AOD) data from the Moderate-resolution Imaging Spectroradiometer (MODIS) satellite indicate that high concentrations of aerosols from intense biomass burning activities in Southeast Asia in March 2006 could be transported to the Guangzhou area by prevailing south-westerly winds (Deng et al., 2008). Huang et al. (2023) employed the WRF-Community Multiscale Air Quality (WRF-CMAQ) model and quantified that the biomass burning emissions in Southeast Asia accounted for 21 % of the surface average $PM_{2.5}$ concentrations in Guangdong Province in March 2015.

Previous studies have shown that the transport of pollutants from BBSEA to southern China is influenced by meteorological conditions (Huang et al., 2023; Yang et al., 2022). The average wind direction in Southeast Asia is from west to east in March, transporting pollutants to the east (Deng et al., 2008). For example, Fu et al. (2012) showed that pollutants on the ground from BBSEA in March were transported to high altitudes by strong convective air, and were rapidly transported eastward over long distances by strong westerly winds at an altitude of around 2 km in the troposphere, which contributed to 30 %–70 % of the high-altitude $PM_{2.5}$ concentrations in the Pearl River Delta (PRD) region on March 27, 2006 by CMAQ model. In April, there was a shift in the wind fields over Southeast Asia, with wind direction changing from west to southwest, which can cause pollutants from biomass burning emissions to be transported to the northeast (Huang et al., 2023).

The methods employed in previous studies to quantify the contributions of regional transport of pollutants by the atmospheric chemical transport models include the tagged tracer method (Chen et al., 2016; Yang et al., 2017), sensitivity simulation experiments (Fan et al., 2023; Li et al., 2016), and adjoint model (Gu et al., 2025; Mao et al., 2020, 2024). The adjoint model can efficiently calculate the sensitivities of pollutant concentrations at the study site to global emissions at the model's spatial and temporal resolution by a single simulation (Gu et al., 2025; Mao et al., 2020; Zhang et al., 2015).

Currently, the annual average $PM_{2.5}$ concentrations in southern China have reached the Grade II of the CAAQS (35 μg m^{-3}), but are still far from the World Health Organization (WHO) Grade III standard (15 μg m^{-3}) (Pang et al., 2023; Wei et al., 2024). With the decline of anthropogenic emissions in China, the impact of BBSEA on air quality in southern China would likely continue to increase under the trend of global warming. In the present study, we quantify the contributions of BBSEA to BC concentrations in southern China (two provincial capitals: Guangzhou, Guangdong Province, and Kunming, Yunnan Province) based on GEOS-Chem global chemical transport model and its adjoint for the spring (March–April) of 2014 and 2019, when Southeast Asia biomass burning emissions are significantly high. By using the adjoint model, the daily contributions of biomass burning emissions to BC contributions in southern China during the severe pollution events are quantified at the model grid resolution. In addition, we combine with the large-scale atmospheric circulation to further elucidate the transport pathways of BBSEA to southern China. Our study would provide reliable scientific support for insight into aerosol sources and contribute to the further improvement of air quality in southern China.

2. Methods

2.1. GEOS-chem and model simulations

In this study, we use the GEOS-Chem atmospheric chemical transport model and its adjoint model (http://geos-chem.org, version 35, last access: April 2, 2025), driven by Modern-Era Retrospective Analysis for Research and Applications, Version 2 (MERRA2) assimilated meteorological data from Goddard Earth Observing System (GEOS) of Aeronautics and Space Administration (NASA). In light of our previous BC modeling studies, we employ 'offline' simulations of carbonaceous aerosols to improve computational efficiency. We use a nested model with a horizontal resolution of 0.5° × 0.625° in the Asian region (60°-150°E, 11°S-55°N), 47 vertical layers, and a temporal resolution of 3 h. The boundary conditions are derived from the GEOS-Chem global simulations with a horizontal resolution of 2° × 2.5°.

The GEOS-Chem simulation of carbonaceous aerosols follows by Park and Jacob (2003), which assumed that 80 % of BC are hydrophobic and hydrophobic aerosols become hydrophilic with an e-folding time of 1.2 days (Park et al., 2005). Additionally, the BC in the model is assumed to be externally mixed with other aerosol species. Tracer advection is computed using a flux-form semi-Lagrangian method (Lin and Rood, 1996), and tracer moist convection follows Allen et al. (1996). The deep convection and shallow convection treatments follow Zhang and McFarlane (1995) and Hack (1994), respectively, and the dry deposition of aerosols uses the series resistance model by Walcek et al. (1986).

We employ the GEOS-Chem model to simulate surface and elevated BC concentrations in China for both 2014 and 2019, and the adjoint model to quantify the contributions of BBSEA to BC concentrations in Guangzhou and Kunming during severe pollution events in March–April 2014 and 2019. The GEOS-Chem adjoint model has been validated to be an effective method for source attribution of $PM_{2.5}$ (Gu et al., 2025; Lee et al., 2017) and BC (Mao et al., 2020; Qi et al., 2017; Xu et al., 2017). The adjoint model offers a computationally efficient method for calculating the contribution of BC concentrations to global emissions at the spatial and temporal resolutions of the model through a single backward simulation. In addition, two sensitivity experiments based on GEOS-Chem are also conducted with/without BBSEA for spring 2014 and 2019 to quantify the average contribution of BBSEA to BC concentrations in southern China.

2.2. Emission inventories

The Community Emissions Data System (CEDS, https://github.com/JGCRI/CEDS/tree/master, last access: February 10, 2025, McDuffie et al., 2020) is used for the global anthropogenic emissions of BC at 0.5° × 0.5° horizontal resolution, and the anthropogenic BC emissions in China are from the Multi-resolution Emission Inventory of China (MEIC, http://www.meicmodel.org/, last access: April 2, 2025, Zheng et al., 2018) at 0.5° × 0.667° horizontal resolution, including residential, industrial, transportation and power sectors. In addition, the anthropogenic emissions of BC from CEDS and MEIC are available for 2013–2019, with a temporal resolution of one month. Biomass burning emissions of BC are from the Global Fire Emissions Database v4 (GEFDv4, https://www.globalfiredata.org/, last access: April 2, 2025, Randerson et al., 2017) for 2013–2019, with a horizontal resolution of 0.25° × 0.25° and a temporal resolution of one day.

Fig. 1 (a) shows the monthly biomass burning emissions of BC in GFEDv4 for Southeast Asia (92°-110°E, 10°-28°N) from 2000 to 2019. The annual biomass burning emissions of BC are 21.60–55.85 Tg in Southeast Asia for 2000–2019, with an annual average of 35.26 Tg. There is a distinct seasonal variation in biomass burning emissions of BC in Southeast Asia, which are high from February to April, accounting for 79 % of the annual biomass burning emissions of BC in the region from 2000 to 2019. In 2014, the annual biomass burning emissions of BC in Southeast Asia reach 46.38 Tg, which is the year with the highest emissions between 2013 and 2019, and with 85 % of the annual emissions occurring from February to April. Fig. 1 (b) shows the daily biomass burning emissions of BC from four sources in Southeast Asia from February to April 2014, and the monthly total emissions from February to April are 638.10 Gg (17 %), 1635.30 Gg (43 %), and 959.79 Gg (25 %), respectively. In addition, Tropical deforestation and degradation (DEFO) in Southeast Asia is the main source of BC emissions, accounting for 45 % of total biomass burning BC emissions in February–April 2014. BC emissions from Savanna, grassland, and shrubland fires (SAVA), Temperate forest fires (TEMP), and Agricultural waste burning (AGRI) correspondingly account for 36 %, 10 %, and 9 %, respectively.

Fig. 2 shows the spatial distribution of BC from biomass burning emissions in the GFEDv4 for 2014 in Asia. In 2014, the annual biomass burning emissions of BC are 46.38 Tg in Southeast Asia and 12.84 Tg in China. High biomass burning emissions are observed in eastern Myanmar, northwest Thailand, northern Laos, and northeast Cambodia. Among these regions, Myanmar and Laos are situated in the upwind zone of the southwest monsoon, and high biomass burning emissions from these areas have the potential to significantly impact air quality in southern China (Zhang et al., 2022).

2.3. MERRA2 reanalysis data

The MERRA2 (https://earthdata.nasa.gov/, last access: April 2, 2025, Gelaro et al., 2017) reanalysis data provides pollutant concentration data, such as $PM_{2.5}$ and BC with a horizontal resolution of 0.5° × 0.625° and 72 vertical layers, based on the GEOS-5 Model (version 5) and Data Assimilation System (version 5.12.4). The Data Assimilation System is used to assimilate AOD from several sources, including MODIS, the High-Resolution Radiometer (AVHRR), the Multi-Angle Imaging Spectroradiometer (MISR), the Aerosol Robotic Network (AERONET), and aircraft observation. In this study, we download hourly surface BC concentrations data for China in 2014 and 2019 from the MERRA2 data.

2.4. ERA5

European Centre for Medium-Range Weather Forecasts Reanalysis version 5 (ERA5, last access: April 2, 2025, https://cds.climate.copernicus.eu/datasets/reanalysis-era5-single-levels?tab=overview) is the fifth generation of reanalysis data, providing a multitude of atmospheric, oceanic, and surface data (Hoffmann et al., 2019). The ERA5 data employs data assimilation techniques to integrate observational data with model simulations, using an optimization method to achieve the best results. The present study utilizes hourly wind fields data at

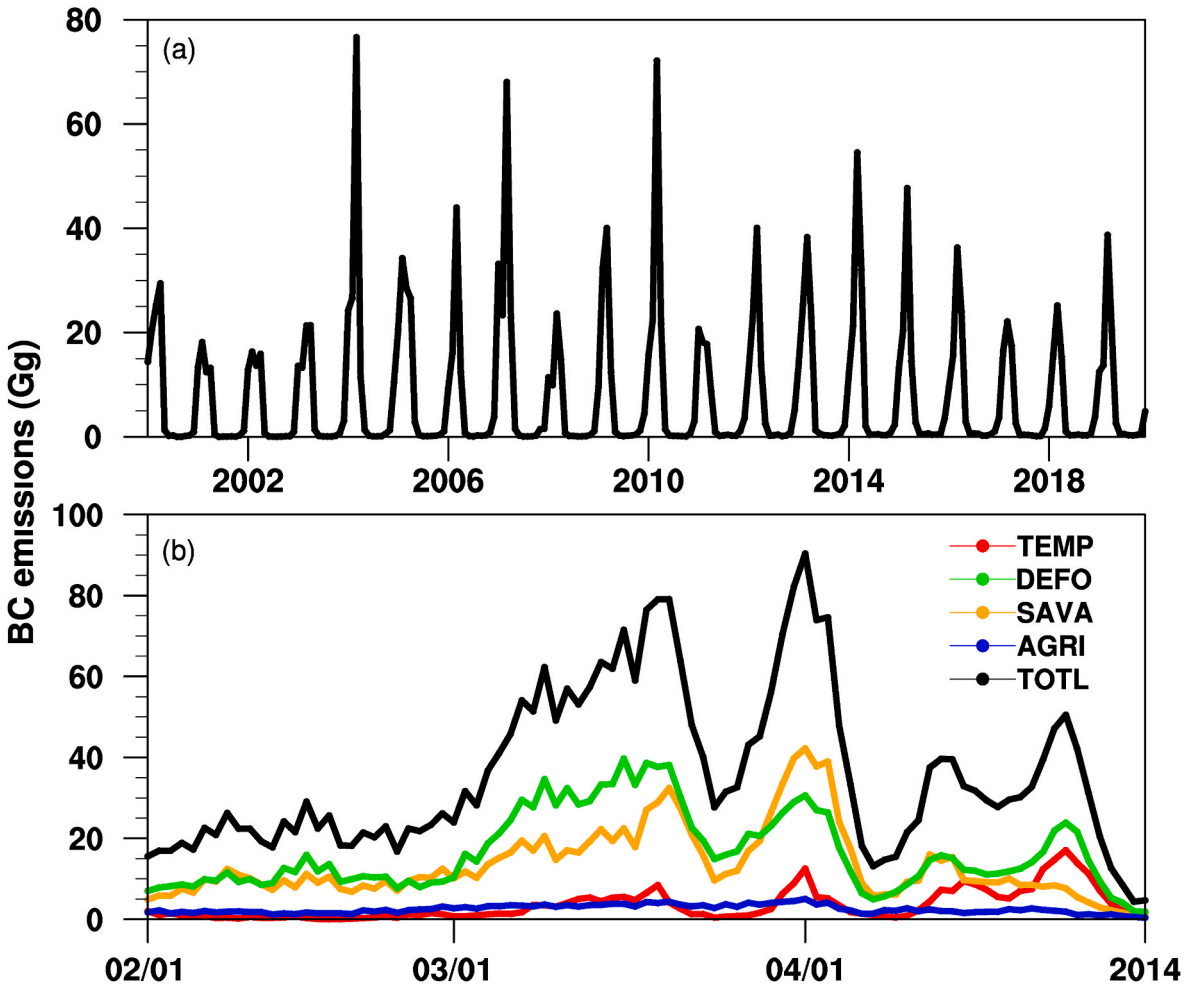

Fig. 1. (a) The monthly biomass burning emissions of BC (Gg) in GFEDv4 in Southeast Asia (92°-110°E, 10°-28°N) from 2000 to 2019. (b) The daily biomass burning emissions of BC from four sources (Temperate forest fires (TEMP), Tropical deforestation and degradation (DEFO), Savanna, grassland, and shrubland fires (SAVA), and Agricultural waste burning (AGRI)) in Southeast Asia from February to April 2014.

ground level and 700 hPa for 2014 and 2019 in the Asian region (0°-50°N, 70°-150°E) from the ERA5 data, with a horizontal resolution of 0.25° × 0.25°. ERA5 data has higher horizontal resolution and vertical resolution than MERRA2 data, which can accommodate more flow features and lead to more realistic flow structures (Wu et al., 2024; Zhang et al., 2016). Furthermore, the difference in mean wind speed between the ERA5 data and observations is smaller than that between the MERRA2 data and observations (Fan et al., 2021; Miao et al., 2020; Wu et al., 2024).

3. Simulated BC and model evaluation

Previous studies have indicated that the GEOS-Chem model could reasonably simulate interannual, seasonal, and daily variations of BC concentrations in China (Chan, 2017; Mao et al., 2016, 2020). As demonstrated in Table 1, we evaluate the reliability of the GEOS-Chem model to simulate BC concentrations in southern China by utilizing observed annual and monthly average surface BC concentrations at seven stations for 2013–2019 from the literature. The deviation of simulations and observations ranges from −19 % to 18 % at most measurement sites, except the Shenzhen site in Guangdong Province (Chen et al., 2022) and the Nanning site in Guangxi Province (Ding et al., 2023). Furthermore, Emery et al. (2017) suggested that the model simulations are acceptable when the normalized mean bias (NMB) between model simulations and observations of BC is within ±20 %. The specific formula is as follows:

$$NMB = \frac{\sum_{i=1}^{N}(C_m - C_o)}{\left(\sum_{i=1}^{N} C_o\right)} \quad (1)$$

where C_m is the simulated BC concentration, C_o is the observed BC concentration, and N is the number of observations. As shown in Fig. 3, the simulations are evaluated using the observed monthly average surface BC concentrations at the Shenzhen site in Guangdong Province in 2014 (Cheng, 2018) and at the Zhaoqing in Guangdong Province in 2019 (Lu et al., 2021). The NMB values between simulated and observed monthly average surface BC concentrations are 7 % at Shenzhen in 2014 and 6 % at Zhaoqing in 2019, and the corresponding correlation coefficients are 0.83 and 0.79, respectively, which are statistically significant with 95 % confidence from a two-tailed Student's t-test.

Previous studies have shown that MERRA2 data can well present the spatial and temporal variations of observed surface BC concentrations in China (Cao et al., 2021; Mao et al., 2023; Xu et al., 2020), and thus MERRA2 data could be used to indirectly validate simulated surface BC concentrations due to the lack of observational data of BC in China (Fang et al., 2020; Hu et al., 2024; Yang et al., 2024; Zhou et al., 2023, 2024). For example, Mao et al. (2023) and Xu et al. (2020) validated the MERRA2 data by using observed surface BC concentrations from 35 stations in China (1981–2020) and 14 stations in eastern China (2000–2016), respectively, and the corresponding correlation coefficients between the MERRA2 and observed monthly average surface BC concentrations were 0.68 and 0.83.

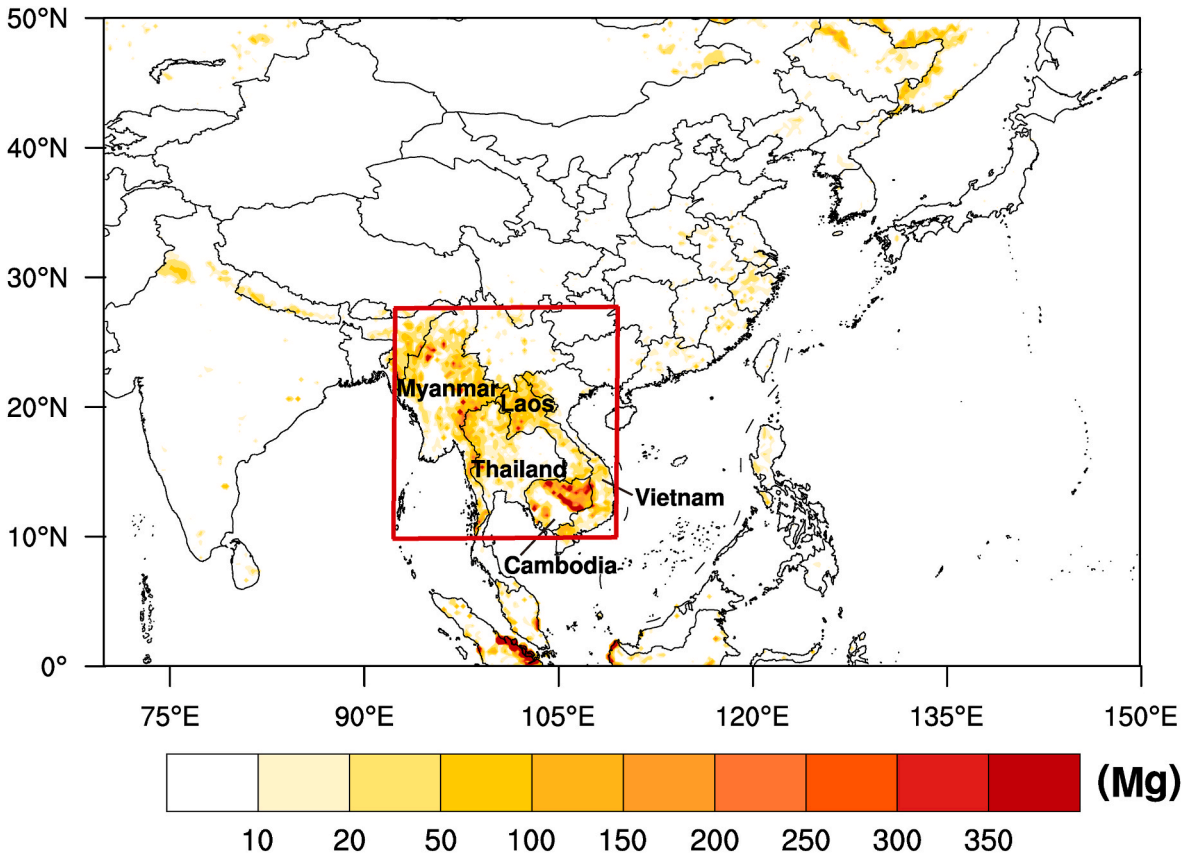

Fig. 2. The spatial distribution of annual biomass burning emissions of BC (Mg) from GFEDv4 in Asia for 2014. The texts in black represent five countries of Myanmar, Thailand, Laos, Vietnam, and Cambodia in Southeast Asia. The red box represents the domain of Southeast Asia (92°-110°E, 10°-28°N). (For interpretation of the references to colour in this figure legend, the reader is referred to the Web version of this article.)

Table 1
Observed and simulated monthly and annual average surface BC concentrations (μg m^{-3}) at 7 sites in China.

Observation site	Observation period	Observation instrument	Observed concentrations	Simulated concentrations	Reference
Shenzhen, Guangdong	2014	AE-31	2.71	2.89	Cheng et al. (2018)
	2019.10–2019.12	AE-33	2.52 ± 1.56	1.77	Chen et al. (2022)
Guangzhou, Guangdong	2013	5012MAAP	3.35	3.06	Lin et al. (2019)
	2019.1	RT-4	1.70 ± 1.20	2.02	Pei et al. (2023)
Zhaoqing, Guangdong	2019	RT-4	1.60	1.32	Lu et al. (2021)
Hongkong	2016.2–2017.1	AE-31	3.2 ± 0.9	2.59	Zhang et al. (2018)
Nanning, Guangxi	2017	AE-31	1.02 ± 0.53	0.76	Ding et al. (2023)

Fig. 4 illustrates the daily average surface BC concentrations from the GEOS-Chem model and MERRA2 data at Guangzhou (Fig. 4 (a)) and Kunming (Fig. 4 (b)) in southern China in 2014. The correlation coefficient between the simulated values and the MERRA2 data is 0.46 at Guangzhou and 0.40 at Kunming, and the corresponding NMB values are 27 % and 47 %, respectively. In this study, the daily average surface BC concentrations from MERRA2 in Guangzhou and Kunming in 2014 are lower than the simulated BC concentrations. Previous studies have shown that the MERRA2 data likely underestimated the surface BC concentrations in China. For example, Li et al. (2024) and Cao et al. (2021) highlighted that the MERRA2 data exhibited a 19 % underestimation of the observed surface BC concentrations at 64 sites in China from 1994 to 2016 and a 29 % underestimation at 34 sites in China from 2006 to 2016, respectively. The underestimation of surface BC concentrations by the MERRA2 data partially results from meteorological and assimilation data (Buchard et al., 2017; Ma et al., 2020). The meteorological data in MERRA2 data overestimate the average wind speed and wind density at the surface of Asia (Carvalho, 2019; Miao et al., 2020). In addition, the satellites used for the assimilation system in MERRA2 data are affected by a combination of cloud blockage and abundant precipitation in southern China, which can result in the absence of AOD data (Buchard et al., 2017; Ma et al., 2020; Qin et al., 2019).

In 2019, the correlation coefficient of the daily average surface BC concentrations between the GEOS-Chem model and MERRA2 data is 0.58 at Guangzhou (Fig. 4 (c)) and 0.62 at Kunming (Fig. 4 (d)), which are higher than those in 2014, and the corresponding NMB values are −38 % and −34 % in 2019, respectively. The daily average surface BC concentrations from MERRA2 in Guangzhou and Kunming in 2019 are higher than the simulated BC concentrations. This discrepancy can be attributed to the outdated anthropogenic BC emissions in MERRA2, and the separation of specific aerosol species in its assimilation system based on the total aerosol optical depth (Buchard et al., 2017; Che et al., 2024; Yang et al., 2024).

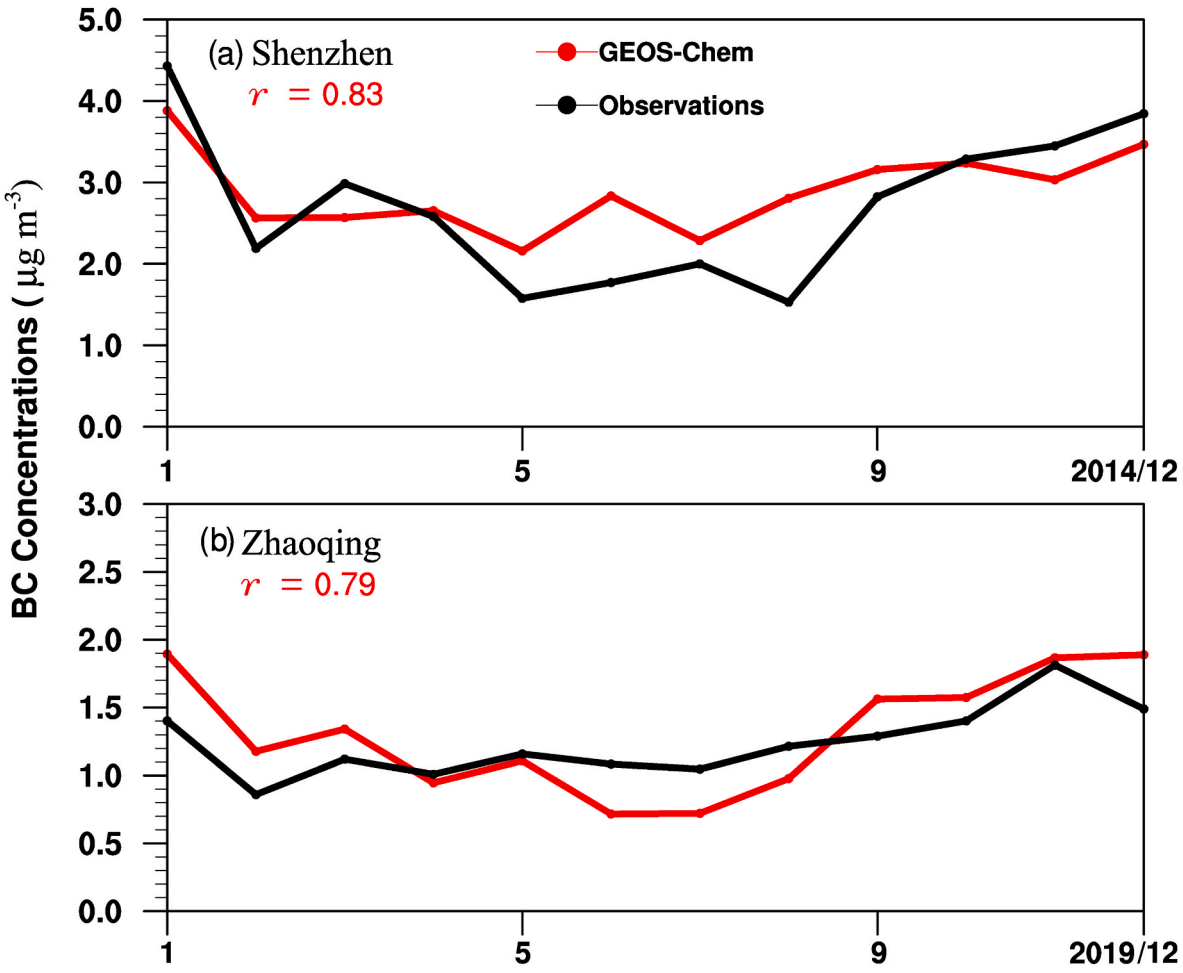

Fig. 3. Observed (black) and GEOS-Chem simulated (red) monthly average surface BC concentrations (μg m^{-3}) and corresponding correlation coefficient (*r*) between simulations and observations of BC concentrations (a) at Shenzhen site for 2014, and (b) at Zhaoqing site for 2019. (For interpretation of the references to colour in this figure legend, the reader is referred to the Web version of this article.)

4. Result

4.1. Source of BC during the pollution events in Guangzhou in 2014

Under the dual scenario of a potential increase in BBSEA and a significant decline in China's anthropogenic emissions, the impact of BBSEA on air quality in southern China may become more pronounced. In order to quantify the influence of high BBSEA on air quality in southern China on heavy pollution events, we select three pollution events with elevated surface BC concentrations in Guangzhou (Guangdong Province) and Kunming (Yunnan Province) between March and April 2014, when the annual total BBSEA are highest for 2013–2019. In 2014, surface daily average BC concentrations in Guangzhou and Kunming are 3.96 μg m^{-3} and 2.14 μg m^{-3} on March 23, 4.15 μg m^{-3} and 1.92 μg m^{-3} on April 5, and 3.59 μg m^{-3} and 2.29 μg m^{-3} on April 17, respectively (Fig. 4 (a) and 4 (b)). During the pollution events of March 23 and April 5, biomass burning emissions are notably high in Southeast Asia. These two cases are specifically selected to further investigate the significance of wind fields, since the wind fields over South Asia exhibit a shift during the event on April 5. For the pollution event of April 17, there is a significant decrease in BBSEA compared to the first two cases. The GEOS-Chem adjoint model is integrated backward for 14 days to obtain the contributions of hourly BC emissions on a 0.5° × 0.625° horizontal grid scale to surface and high-altitude BC concentrations during the three pollution events in Guangzhou and Kunming. The discrepancies between the surface and high-altitude BC concentrations simulated by the adjoint and forward models for the three pollution events in Guangzhou and Kunming are below ±15 %.

Fig. 5 illustrates the daily contributions of anthropogenic emissions, biomass burning emissions, and BBSEA to the daily average BC concentrations at the surface and 700 hPa in Guangzhou during the three pollution events. Fig. S1 shows the spatial distributions of the contributions from anthropogenic and biomass burning emissions, which are integrated backward for 14 days. During the pollution event in Guangzhou on March 23, 2014, as shown in Fig. 5 (a1), the total backward 14-day contributions of anthropogenic emissions and biomass burning emissions to the daily average surface BC concentrations in Guangzhou on March 23 are 3.38 μg m^{-3} (94 %) and 0.21 μg m^{-3} (6 %), respectively. Anthropogenic emissions mainly originate from Guangzhou and southern Fujian Province (Fig. S1 (a1)), with the impacts that amount to 2.68 μg m^{-3} (75 %) and 0.19 μg m^{-3} (5 %) of the daily average surface BC concentrations. The anthropogenic BC emitted from outside Guangzhou is transported by northeasterly winds over 2–7 days to the surface of Guangzhou. The BBSEA (Fig. S1 (a2)) are primarily from southeastern Myanmar, which account for 0.19 μg m^{-3} (5 %) of the daily average surface BC concentrations, and take approximately 3–6 days to reach the surface in Guangzhou. Observed from Ozone Mapping and Profiler Suite satellite (OMPS), Zhang et al. (2022) also found that serious air pollution from BBSEA in March would transport to Guangdong Province in 3–6 days.

Previous studies have shown that the major pathway for transporting pollutants emitted from BBSEA to southern China is around 700 hPa

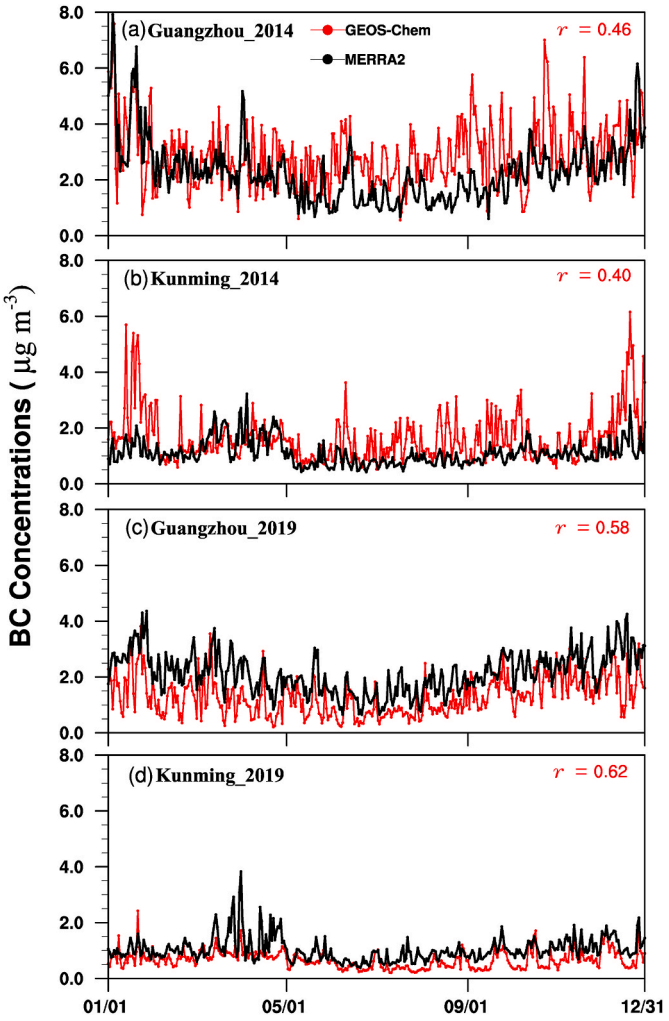

Fig. 4. GEOS-Chem simulated (red) and MERRA2 reanalysis (black) daily average surface BC concentrations (μg m^{-3}) and corresponding correlation coefficient (*r*) between simulations and reanalysis of BC concentrations (a) at Guangzhou site for 2014, (b) at Kunming site for 2014, (c) at Guangzhou site for 2019, and (d) at Kunming site for 2019. (For interpretation of the references to colour in this figure legend, the reader is referred to the Web version of this article.)

(Lian et al., 2024; Yang et al., 2022), where these pollutants are influenced by south-westerly winds from the source area through the South China Sea and eventually reach Guangdong Province (Zhang et al., 2022). Fig. 5 (a2) shows the daily contributions of anthropogenic emissions and BBSEA to the daily average BC concentrations at 700 hPa in Guangzhou on March 23, 2014, which amount to 0.20 μg m^{-3} (27 %) and 0.55 μg m^{-3} (73 %), respectively, over the past 14 days. Fig. 6 (a1) and 6 (a2) show the spatial distributions of the total backward 14-day contributions from anthropogenic emissions and biomass burning emissions to the daily average BC concentrations at 700 hPa in Guangzhou. At 700 hPa, the majority of anthropogenic emissions are attributable to northern Thailand, emanating from a combination of residential, industrial, and transportation sources (Fig. 6 (a1)). As shown in Fig. 6 (a2), the contributions of local biomass burning emissions to the daily average BC concentration at 700 hPa in Guangzhou are negligible, as most biomass burning emissions originate from Southeast Asia, particularly southeastern Myanmar and northwestern Thailand. The transport of BC emitted from biomass burning in southeastern Myanmar and northwestern Thailand to high altitudes in Guangzhou is facilitated by strong southwesterly winds at 700 hPa within the latitudinal range of 15°N to 25°N. As shown in Fig. 5 (a1) and (a2), the relative percentage contribution of BBSEA to the daily average BC concentrations at 700 hPa is significantly larger than that to the surface BC. BC emitted from BBSEA takes approximately 2–6 days to reach the 700 hPa in Guangzhou, which is shorter than the time required to transport to the surface.

The results of the sensitivity experiments show that the impacts of BBSEA on BC concentrations are 0.12 μg m^{-3} (6 %) at the surface and 0.43 μg m^{-3} (48 %) at 700 hPa in Guangzhou during March–April 2014 (Fig. S2 (a)). Both results of sensitivity experiments and adjoint modeling indicate that BBSEA contribute more BC concentrations at high altitudes than at the surface in Guangzhou. The results of our study are similar to those from the previous studies, for example, Li et al. (2022) used the Regional Integrated Earth Modeling System with Chemistry model (RIEMS-Chem) to find that the relative contributions of BBSEA to the high-altitude BC concentrations in Guangzhou were higher than those to the surface BC concentrations during March 2019. Fang et al. (2020) also showed that the contribution of BBSEA was 6 % to the surface mean BC concentrations in Guangdong Province from March to May 2000–2014, and 44 % to the mean BC concentrations at 750 hPa, by using the Community Earth System Model (CEMS). The BC emitted from BBSEA was transported to the high altitude in Guangzhou by the south-westerly wind and then increased the BC concentrations at the surface through the vertical mixing of the turbulent flow (Fu et al., 2012; Huang et al., 2023; Li et al., 2022).

We then quantify the contribution of BBSEA to surface and high-altitude BC concentrations in Guangzhou on April 5, 2014, to investigate the effects of the wind fields. Fig. 5 (b1) shows that the total backward 14-day contributions of anthropogenic emissions, biomass burning emissions, and BBSEA to the daily average surface BC concentrations in Guangzhou on April 5 are 3.46 μg m^{-3} (94 %), 0.22 μg m^{-3} (6 %), and 0.08 μg m^{-3} (2 %), respectively. Anthropogenic emissions are mainly concentrated in Guangzhou and southern Fujian Province (Fig. S1 (b1)), while biomass burning emissions are largely from AGRI and SAVA in Guangzhou (Fig. S1 (b2)), which account for 0.14 μg m^{-3} (4 %) of surface daily average BC concentrations. At 700 hPa, anthropogenic emissions and BBSEA supply 0.34 μg m^{-3} (30 %) and 0.78 μg m^{-3} (70 %) of the daily average BC concentrations in Guangzhou on April 5 (Fig. 5 (b2)). As shown in Fig. 6 (b1) and (b2), anthropogenic emissions are primarily from Guangxi Province and Vietnam, while biomass burning emissions predominantly originate from eastern Myanmar and northern Laos. The absolute contribution of BBSEA to BC concentrations at 700 hPa in Guangzhou on April 5 is 0.78 μg m^{-3}, which exceeds the corresponding contribution of 0.55 μg m^{-3} on March 23. It is noteworthy that the total BC emissions from BBSEA during the initial 14-day period of the pollution event on April 5 (727.16 Gg) are less than those on March 23 (837.72 Gg). During the pollution event on April 5, more BC from BBSEA are transported to Guangzhou, and the transport time shorten by about 1 day, which is likely due to stronger wind speeds and a shift in wind direction from southwest to west at 700 hPa in Southeast Asia, compared to the pollution event on March 23 (Fig. 6 (a2)). By using RAQMS, Li et al. (2024) reported that the transport of BBSEA to the high altitude of Guangdong province would be enhanced under stronger westerly winds from South Asia in 2010 compared to other years in 2009–2018.

On April 17, 2014, the total emissions of BC from BBSEA over the preceding 14 days amount to 379 Gg, marking a significant decrease compared to the previous two cases. Fig. 5 (c1) shows that anthropogenic emissions, biomass burning emissions, and BBSEA over the past 14 days contribute 2.88 μg m^{-3} (96 %), 0.12 μg m^{-3} (4 %), and 0.10 μg m^{-3} (3 %), respectively, to the daily surface mean BC concentrations in Guangzhou on April 17. Anthropogenic emissions are largely from Guangzhou (Fig. S1 (c1)), while biomass burning emissions are mainly concentrated in the northern Laos (Fig. S1 (c2)). At 700 hPa (Fig. 5 (c2)), anthropogenic emissions, predominantly originating from central Myanmar (Fig. 6 (c1)), contribute to 0.13 μg m^{-3} (38 %) of daily average BC concentrations; biomass burning emissions from Southeast Asia, mainly from northern Myanmar (Fig. 6 (c2)), account for 0.20 μg m^{-3}

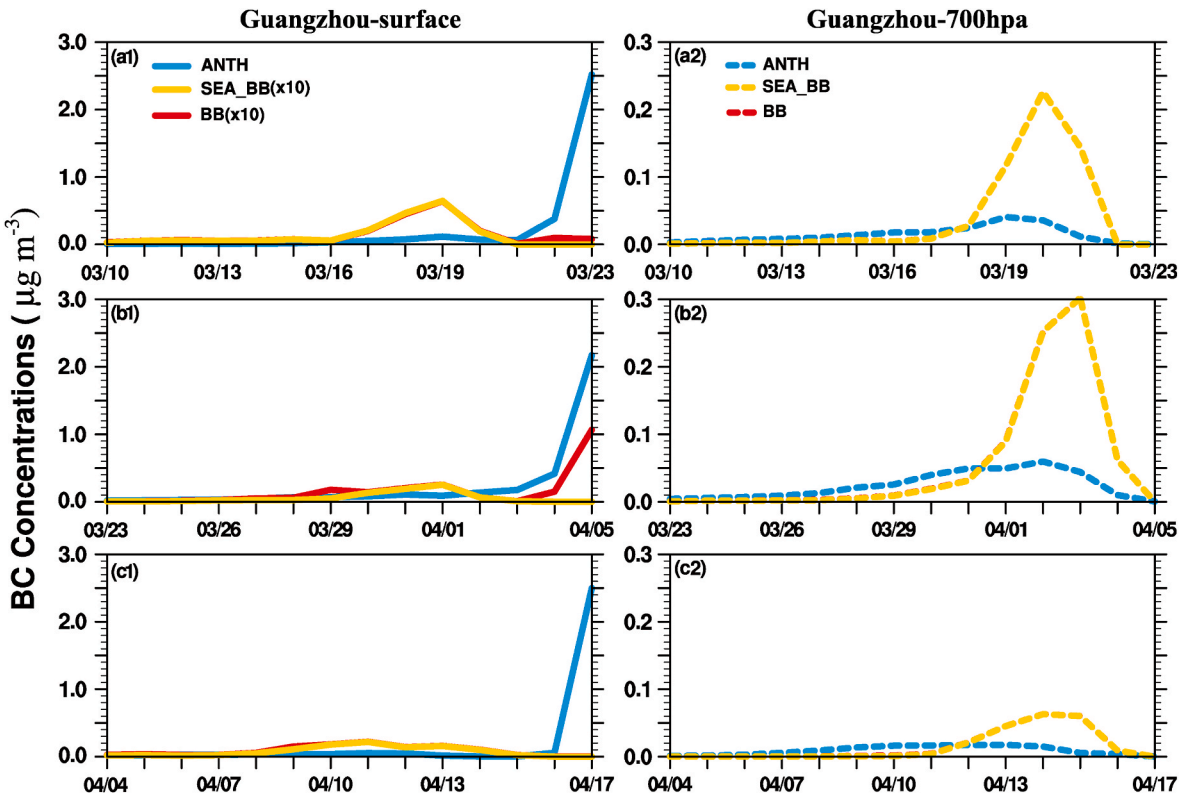

Fig. 5. Time-dependent daily contributions to daily average BC concentrations (μg m^{-3}, going backward for 14 days) at the surface (left panel) and at 700 hPa (right panel) in Guangzhou from anthropogenic emissions (ANTH), biomass burning emissions (BB), and biomass burning emissions from Southeast Asia (SEA_BB). Results are computed by the GEOS-Chem adjoint model for three pollution events: (a) March 23, 2014, (b) April 5, 2014, and (c) April 17, 2014.

(59 %) of BC concentrations. To compare with the previous two cases, the contribution of BBSEA to the BC concentrations at 700 hPa in Guangzhou decrease during the pollution event on April 17, due to the reduction in biomass burning emissions from Southeast Asia.

4.2. *Source of BC during the pollution events in Kunming in 2014*

We further analyze the impact of BBSEA on BC concentrations in Kunming, Yunnan Province, as Kunming is in proximity to Southeast Asia. Fig. 7 shows the daily contributions of anthropogenic emissions, biomass burning emissions, and BBSEA to the daily average BC concentrations at the surface and 700 hPa in Kunming during the three pollution events. The correspondingly spatial distributions of the contributions from anthropogenic emissions and biomass burning emissions are shown in Fig. S3. On March 23, 2014, as shown in Fig. 7 (a1), the impact of anthropogenic emissions, biomass burning emissions, and BBSEA on the surface daily average BC concentrations in Kunming over the past 14 days reaches 0.96 μg m^{-3} (68 %), 0.45 μg m^{-3} (32 %), and 0.44 μg m^{-3} (31 %), respectively. Anthropogenic emissions are largely from Kunming (Fig. S3 (a1)), while biomass burning emissions mainly come from southeastern Myanmar and northern Thailand (Fig. S3 (a2)). Furthermore, it takes approximately 1–5 days for the BC emitted from BBSEA to be transported to the surface in Kunming. Li et al. (2022) also showed that strong biomass burning emissions from Thailand could transport to the surface in Kunming in 1–2 days by using the RIEMS-Chem model.

Notably, the total contributions of BBSEA to surface daily average BC concentrations in Kunming are significantly higher than those in Guangzhou (Fig. 5 (a1)). Previous studies have indicated that BBSEA significantly contribute to surface BC concentrations in Kunming, due to Kunming's proximity to Southeast Asia and its high altitudes (Huang et al., 2023; Lian et al., 2024; Yang et al., 2022). Lian et al. (2024) employed the Whole Atmosphere Community Climate model (WACCM) to demonstrate that the pollutants from BBSEA were lifted by atmospheric currents to about 700 hPa and could be rapidly deposited on the surface of Kunming.

At 700 hPa, as shown in Fig. 7 (a2), anthropogenic emissions and BBSEA account for 0.55 μg m^{-3} (56 %) and 0.43 μg m^{-3} (44 %) of the daily average BC concentrations in Kunming on March 23. Anthropogenic emissions are mainly from Kunming, southern Myanmar, and northern Thailand (Fig. S3 (a3)), while biomass burning emissions are principally from eastern Myanmar and northern Thailand (Fig. S3 (a4)). In addition, it takes about 1–5 days for the BC emitted from BBSEA to be transported to high altitude in Kunming. The BC emitted from BBSEA, particularly Myanmar, is transported across the China-Myanmar border by strong southwesterly winds and reaches high altitudes over Kunming. Yang et al. (2022) used WRF-Chem to find that the percentage contribution of BBSEA was 37 % to the surface average $PM_{2.5}$ concentrations in Kunming during the period from March 24 to 26, 2017, with the main source of BBSEA being eastern Myanmar. Sensitivity experiments show that the impacts of BBSEA on BC concentrations in Kunming during March–April 2014 is 0.39 μg m^{-3} (28 %) at the surface and 0.32 μg m^{-3} (37 %) at 700 hPa (Fig. S2 (b)). The relative contribution of BBSEA to the BC concentration at 700 hPa also exceeds that at the surface in Kunming, a pattern similar to the simulated results in Guangzhou.

The impact of BBSEA on the BC concentrations in Kunming is also influenced by the wind fields. On April 5, 2014, as illustrated in Fig. 7 (b1) and (b2), the total contributions of anthropogenic emissions, biomass burning emissions, and BBSEA to the surface daily average BC concentrations are 0.94 μg m^{-3} (57 %), 0.71 μg m^{-3} (43 %), and 0.54 μg m^{-3} (33 %), respectively, and the corresponding contributions at 700 hPa are 0.56 μg m^{-3} (55 %), 0.45 μg m^{-3} (45 %) and 0.45 μg m^{-3} (45 %), respectively. On the ground, anthropogenic emissions are mainly concentrated in Kunming and western Myanmar (Fig. S3 (b1)), while biomass burning emissions are primarily from Kunming, northeastern, and western Myanmar (Fig. S3 (b2)). Notably, the biomass burning

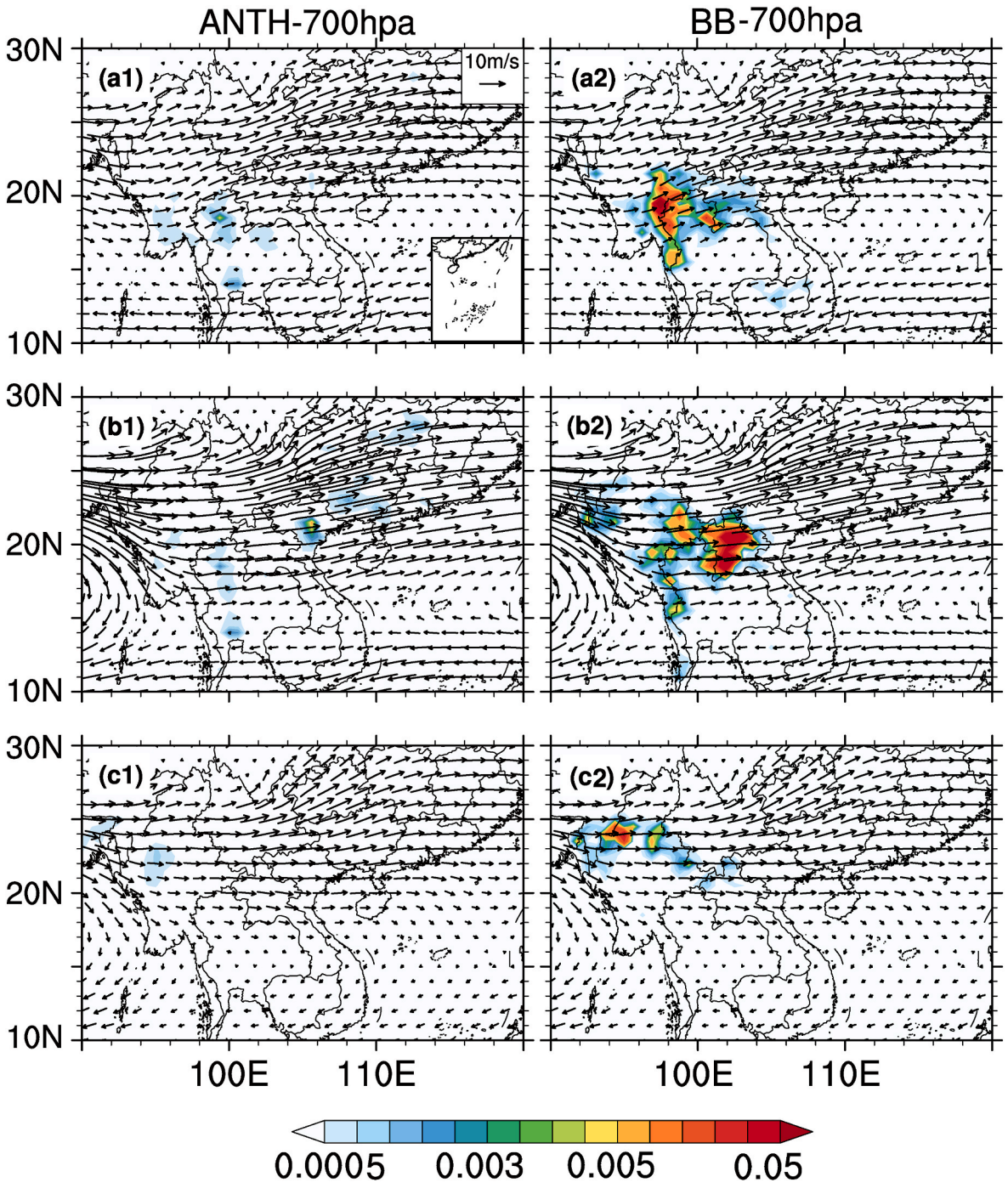

Fig. 6. The spatial distributions of the total contributions to daily average BC concentrations (μg m^{-3}, going backward for 14 days) at 700 hPa in Guangzhou from anthropogenic and biomass burning emissions computed by the GEOS-Chem adjoint model integrated over (a) March 10–23, 2014, (b) March 23-April 5, 2014, and (c) April 4–17, 2014. Corresponding wind fields (m s^{-1}) at 700 hPa are from ERA5 data.

emissions are largely attributed to AGRI, SAVA, and TEMP sectors in Kunming. At 700 hPa, the impact of BBSEA on high-altitude BC concentrations over Kunming occurs in less than 1 day. We find that the stronger southwesterly winds over South Asia lead to a higher absolute contribution of BBSEA to the BC concentrations in Kunming on April 5 and a shorter transport time compared to that on March 23, which is similar to the simulation results in Guangzhou. Furthermore, unlike the results from Guangzhou, the primary sources of biomass burning emissions exclude northern Laos during the pollution event in Kunming on April 5, primarily because Kunming is not located in the downwind direction from northern Laos (Fig. S3 (b4)).

We further investigate the impact on BC concentrations in Kunming, when BBSEA decline. Specifically, compared to the previous two cases, the total BBSEA declined over the 14 days preceding April 17, 2014. As shown in Fig. 7 (c1) and (c2) anthropogenic emissions, biomass burning emissions, and BBSEA contribute to 1.24 μg m^{-3} (71 %), 0.50 μg m^{-3} (29 %), and 0.27 μg m^{-3} (15 %) of the surface daily average BC concentrations in Kunming on April 17, respectively. Correspondingly, at 700 hPa, these contributions are 0.61 μg m^{-3} (67 %), 0.30 μg m^{-3} (33 %), and 0.25 μg m^{-3} (28 %), respectively. At the surface, anthropogenic emissions are mainly from Kunming, western Yunnan Province, and Bangladesh (Fig. S3 (c1)), while biomass burning emissions are largely

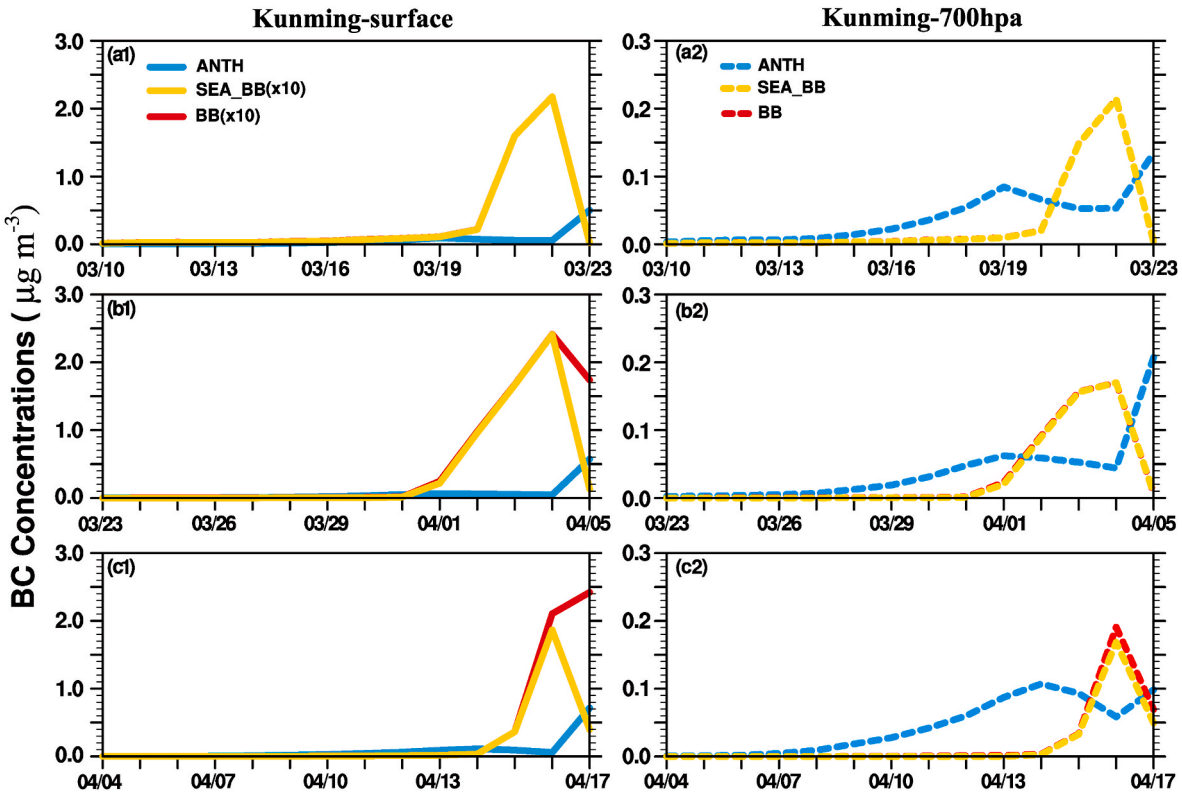

Fig. 7. Same as Fig. 5, but for contributions to daily average BC concentrations in Kunming.

from Kunming and northern Myanmar (Fig. S3 (c2)). It is noted that, compared with the previous two cases, the contribution of BBSEA to BC concentrations at high altitudes in Kunming on April 17 decreases, which is similar to the simulation results in Guangzhou (Fig. 5 (c2)).

4.3. Source of BC during the pollution event in 2019

Since the implementation of the Action Plan for the Prevention and Control of Air Pollution in 2013, followed by the Three-Year Action Plan for Winning the Battle for the Blue Sky in 2018, the $PM_{2.5}$ concentrations have decreased by approximately 48 % in China (Geng et al., 2024). There has also been a significant reduction in BC concentrations in southern China, for instance, the annual average surface BC concentrations in Guangzhou decreased from 3.35 μg m^{-3} in 2013 to 1.59 μg m^{-3} in 2019 (Lin et al., 2019; Pei et al., 2023). We find that anthropogenic BC emissions in the MEIC have declined from 1713.74 Gg in 2013 to 1023.36 Gg in 2019 in China. Consequently, given the substantial decline in anthropogenic BC emissions in southern China from 2013, the high BBSEA are likely to have higher contributions to BC concentrations in southern China.

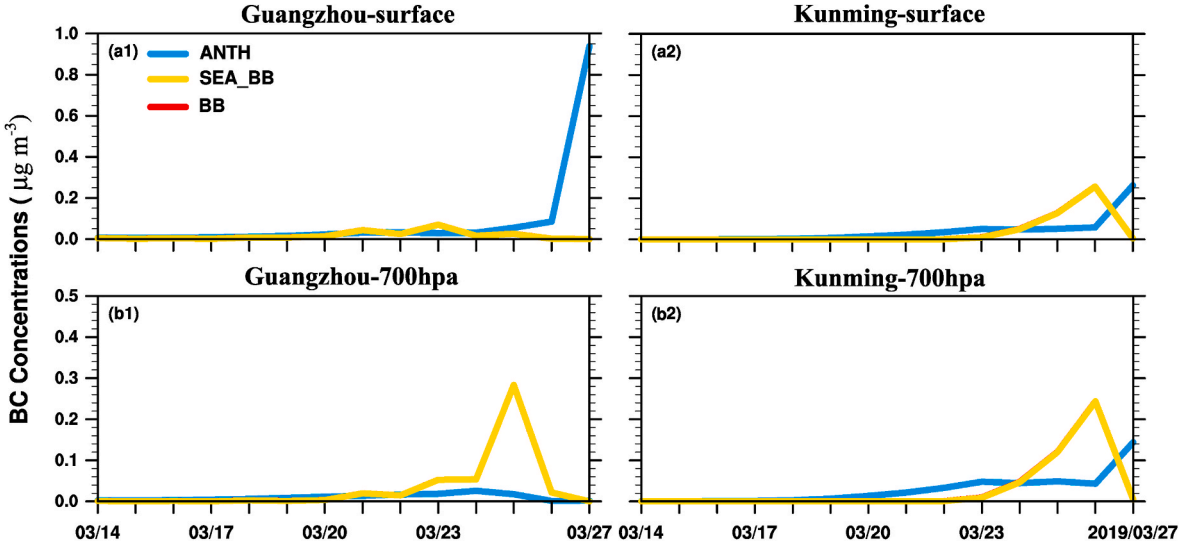

Fig. 8. (left panel) Time-dependent daily contributions to daily average BC concentrations (μg m^{-3}, going backward for 14 days) in Guangzhou at the surface (a1) and at 700 hPa (b1) from anthropogenic emissions (ANTH), biomass burning emissions (BB), and biomass burning emissions from Southeast Asia (SEA_BB) on March 27, 2019. (right panel) same as left panel, but for contributions to daily average BC concentrations in Kunming.

As shown in Fig. 8 (a1) and (b1), the total contributions of anthropogenic emissions and BBSEA to surface daily average BC concentrations in Guangzhou on March 27, 2019, are 1.28 μg m^{-3} (85 %) and 0.22 μg m^{-3} (15 %), respectively, and the corresponding contributions at 700 hPa are 0.13 μg m^{-3} (23 %) and 0.45 μg m^{-3} (77 %), respectively. Anthropogenic emissions originate from Guangzhou (Fig. S4 (a1) and (a3)), while biomass burning emissions mainly come from eastern Myanmar and Northern Laos (Fig. S4 (a2) and (a4)). Our study is similar to the study by Li et al. (2022), which showed that BBSEA accounted for approximately 50 %–70 % of BC column concentrations in southern China in March 2019, by using the RIEMS-Chem model. Additionally, in Kunming, anthropogenic emissions and BBSEA account for 0.56 μg m^{-3} (55 %) and 0.45 μg m^{-3} (45 %), respectively, of surface daily average BC concentrations on March 27, 2019. Correspondingly, at 700 hPa, these emissions contribute 0.41 μg m^{-3} (49 %) and 0.43 μg m^{-3} (51 %), respectively. Anthropogenic emissions largely emanate from Kunming and western Myanmar (Fig. S4 (b1) and (b3)), while biomass burning emissions mainly come from Kunming and central and western Myanmar (Fig. S4 (b2) and (b4)). Fan et al. (2023) also found that western Myanmar is the main biomass burning source, accounting for 76 % of $PM_{2.5}$ concentrations at high altitudes in Kunming from March 28 to April 2, 2019. In addition, as shown in Fig. S2 (c) and (d), the sensitivity experiments show that the contributions of BBSEA to surface BC concentrations in Guangzhou and Kunming during March–April 2019 are 0.09 μg m^{-3} (8 %) and 0.22 μg m^{-3} (25 %), respectively, and the corresponding values at 700 hPa are 0.21 μg m^{-3} (39 %) and 0.11 μg m^{-3} (21 %), respectively.

In this study, the biomass burning emissions of BC in Southeast Asia decrease from 2618.70 Gg in March–April 2014 to 1792.17 Gg in 2019, the absolute contribute of BBSEA to BC in southern China in spring 2019 thus declines. However, the relative contribute of BBSEA on BC concentrations in southern China during the heavy pollution events increases due to a significant reduction in anthropogenic emissions in China. We find that the total BC emissions from BBSEA during the initial 14-day period of the pollution event on March 27, 2019 (599.75 Gg) are less than those on March 23, 2014 (837.72 Gg). However, the percentage contributions of BBSEA to the surface average BC concentrations in Guangzhou and Kunming on March 27, 2019 are 10 % and 14 %, respectively, higher than those on March 23, 2014. Our finding is similar to the study by Zhu et al. (2024), which showed that the contribution of BBSEA to surface monthly average BC concentrations in southern China from March to May increased by 0.4 % from 2013 to 2019 by the GEOS-Chem model.

5. Conclusions

The present study employed the GEOS-Chem and its adjoint model to quantify the contributions of BBSEA to BC concentrations in southern China for the spring of 2014 and 2019. We used surface observations and MERRA2 reanalysis data for model evaluation. The model reasonably represented the variation in surface BC concentrations in two provincial capitals (Guangzhou and Kunming) in southern China.

The results of the adjoint model showed that the contributions of BBSEA to surface daily average BC concentrations in Guangzhou were 0.08–0.19 μg m^{-3} (2 %–5 %) during the three pollution events in March and April 2014, and BBSEA had a significant impact on daily average BC concentrations at 700 hPa in Guangzhou, reaching 0.20–0.78 μg m^{-3} (59 %–73 %). In Kunming, BBSEA contributed to 0.27–0.54 μg m^{-3} (15 %–33 %) of the surface daily average BC concentrations during the three pollution events in 2014. Correspondingly, the contributions were 0.25–0.45 μg m^{-3} (28 %–45 %) at 700 hPa in Kunming. During the pollution event on March 23, 2014, the transport time of biomass burning emissions from Southeast Asia to the surface in Guangzhou (Kunming) was approximately 3–6 days (1–5 days), while the transport time to high-altitude in Guangzhou (Kunming) was 2–6 days (1–5 days). During the pollution event on April 5, 2014, the transport time of biomass burning emissions from Southeast Asia to high-altitude in Guangzhou and Kunming shortened by about 1 day, due to a shift in wind fields (from southwest to west) combined with stronger wind speeds, compared to March 23, 2014.

Since 2013, China's efforts to control air pollution have led to a decline in anthropogenic emissions and aerosol concentrations, while the influence of BBSEA on BC concentrations in southern China has been rising. In 2019, the contributions of BBSEA to surface daily average BC concentrations during the pollution event on March 27 were 0.22 μg m^{-3} (15 %) in Guangzhou and 0.45 μg m^{-3} (45 %) in Kunming. Compared to the pollution case on March 23, 2014, the percentage contributions of BBSEA to daily average BC concentrations at the surface and 700 hPa increased by 10 % and 4 % in Guangzhou, and by 14 % and 7 % in Kunming on March 27, 2019.

In the present study, the uncertainties in source attribution of BC using the adjoint model likely from the accuracy of model simulation, e.g., the resolution of the model and emissions inventory. As China's anthropogenic emissions continue to decrease, the contribution of BBSEA will increase, particularly in the context of global warming, which would hinder further improvements in air quality in southern China. This study would provide a scientific basis for understanding BC sources and facilitating the reduction of $PM_{2.5}$ concentrations to reach the WHO-III standard (15 μg m^{-3}) in southern China.

CRediT authorship contribution statement

Luhang Liu: Writing – original draft, Visualization, Investigation, Data curation. **Yu-Hao Mao:** Writing – review & editing, Methodology, Conceptualization. **Hong Liao:** Conceptualization.

Declaration of competing interest

The authors declare that they have no known competing financial interests or personal relationships that could have appeared to influence the work reported in this paper.

Acknowledgments

This work was supported by the Innovative Research Group Project of National Natural Science Foundation of China (grant no. 42021004) and Natural Science Foundation of Jiangsu Province (grant no. BK20220031). We acknowledge the High-Performance Computing Centre of Nanjing University of Information Science and Technology for their support of this work.

Appendix A. Supplementary data

Supplementary data to this article can be found online at https://doi.org/10.1016/j.atmosenv.2025.121352.

Data availability

Data will be made available on request.

References

Allen, D.J., Rood, R.B., Thompson, A.M., Hudson, R.D., 1996. Three-dimensional radon 222 calculations using assimilated metrological data and a convective mixing algorithm. Geophys. Res. 101, 6871–6881.

Andreae, M.O., 2019. Emission of trace gases and aerosols from biomass burning–an updated assessment. Atmos. Chem. Phys. 19, 8523–8546.

Buchard, V., Randles, C.A., Daslva, A.M., Darmenov, A., Colarco, P.R., Govindaraju, R., Ferrare, R., Hair, J., Beyersdorf, A.J., Ziemba, L.D., Yu, H., 2017. The MERRA-2 aerosol reanalysis, 1980 onward. Part II: evaluation and case studies. J. Clim. 30, 6851–6872.

Cao, S., Zhang, S., Cao, C., Gao, C., Yan, Y., Bao, J., Su, L., Liu, M., Peng, N., Liu, M., 2021. A long-term analysis of atmospheric black carbon MERRA-2 concentration over China during 1980–2019. Atmos. Environ. 264, 118662.

Carvalho, D., 2019. An assessment of NASA's GMAO MERRA-2 reanalysis surface winds. J. Clim. 32, 8261–8281.
Chan, K., 2017. Biomass burning sources and their contributions to the local air quality in Hong Kong. Sci. Total Environ. 596–597, 212–221.
Che, H., Xia, X., Zhao, H., Li, L., Gui, K., Zheng, Y., Song, J., Qi, B., Zhu, J., Miao, Y., Wang, Y., Wang, Z., Wang, H., Dubovik, O., Holben, B., Chen, H., Shi, G., Zhang, X., 2024. Aerosol optical and radiative properties and their environmental effects in China: a review. Earth Sci. Rev. 248, 104634.
Chen, Y., Schleicher, N., Fricker, M., Cen, K., Liu, X.-L., Kaminski, U., Yu, Y., Wu, X.-F., Norra, S., 2016. Long-term variation of black carbon and $PM_{2.5}$ in Beijing, China with respect to meteorological conditions and governmental measures. Environ. Pollut. 212, 269–278.
Chen, W., Cao, X., Ran, H., Chen, T., Yang, B., Zheng, X., 2022. Concentration and source allocation of black carbon by AE-33 model in urban area of Shenzhen, southern China. J. Environ. Health Sci. Eng. 20, 469–483.
Cheng, D., 2018. Characteristics of Black Carbon Aerosol and its Influencing Factors in Typical Cites of the PRD.
Deng, X., Tie, X., Zhou, X., Wu, D., Zhong, L., Tan, H., Li, F., Huang, X., Bi, X., Deng, T., 2008. Effects of Southeast Asia biomass burning on aerosols and ozone concentrations over the Pearl River Delta (PRD) region. Atmos. Environ. 42, 8493–8501.
Ding, S., Liu, D., Zhao, D., Tian, P., Huang, M., Ding, D., 2023. Characteristics of atmospheric black carbon and its wet scavenging in Nanning, South China. Sci. Total Environ. 904, 166747.
Emery, C., Liu, Z., Russell, A.G., Odman, M.T., 2017. Recommendations on statistics and benchmarks to assess photochemical model performance. J. Air Waste Manage 67, 582–598.
Fan, W., Liu, Y., Chappell, A., 2021. Evaluation of global reanalysis land surface wind speed trends to support wind energy development using in situ observations. J. Clim. Appl. Meteorol. 60, 33–50.
Fan, W., Li, J., Han, Z., Wu, J., Zhang, S., Zhang, C., Li, J., 2023. Impacts of biomass burning in Southeast Asia on aerosols over the low-latitude plateau in China: an analysis of a typical pollution event. Front. Environ. Sci. 11, 1101745.
Fang, C., Zhu, B., Pan, C., Yun, X., Ding, D., Tao, S., 2020. Regional and sectoral sources for black carbon over south China in spring and their sensitivity to east asian summer monsoon onset. J. Geophys. Res. Atmos. 125, e2020JD033219.
Fu, J.S., Hsu, N.C., Gao, Y., Huang, K., Li, C., Lin, N., Tsay, S., 2012. Evaluating the influences of biomass burning during 2006 BASE-ASIA: a regional chemical transport modeling. Atmos. Chem. Phys. 12, 3837–3855.
Fu, T.-M., Jian, Y., 2014. Injection heights of springtime biomass-burning plumes over peninsular Southeast Asia and their impacts on long-range pollutant transport. Atmos. Chem. Phys. 14, 3977–3989.
Gelaro, R., Mccarty, W., Suarez, M., Todling, R., Molod, A., Takacs, L., Randles, C., Darmenov, A., Bosilovich, G., Reichl, R., Wargan, K., Coy, L., Cullather, R., Draper, C., Akella, S., Buchard, V., Conaty, A., Silva, A., Gu, W., Kim, G., Koster, R., Lucchesi, R., Merkova, D., Nielsen, J., Partyka, G., Pawson, S., Putman, W., Rienecker, M., Schubert, S., Sienkiewicz, M., Zhao, B., 2017. The Modern-Era Retrospective analysis for Research and Applications, version 2 (MERRA-2). J. Clim. 30, 5419–5454.
Geng, X., Hu, J., Zhang, Z., Li, Z., Chen, C., Wang, Y., Zhang, Z., Zhong, Y., 2024. Exploring efficient strategies for air quality improvement in China based on its regional characteristics and interannual evolution of $PM_{2.5}$ pollution. Environ. Res. 252, 119009.
Gu, Y., Henze, D., Liao, H., 2025. Sources of $PM_{2.5}$ exposure and health benefits of clean air actions in Shanghai. Environ. Int. 195, 109259.
Hack, J.J., 1994. Parameterization of moist convection in the National Center for Atmospheric Research community climate model (CCM2). J. Geophys. Res. Atmos. 99 (D3), 5551–5568.
Hoffmann, L., Gunther, G., Li, D., 2019. From ERA-Interim to ERA5: the considerable impact of ECMWF's next-generation reanalysis on Lagrangian transport simulations. Atmos. Chem. Phys. 19, 3097–3124.
Hu, Y., Yu, H., Kang, S., Yang, J., Rai, M., Yin, X., Chen, X., Chen, P., 2024. Aerosol–meteorology feedback diminishes the transboundary transport of black carbon into the Tibetan Plateau. Atmos. Chem. Phys. 24, 85–107.
Hu, Y., Kang, S., Yang, J., Chen, X., Ji, Z., Rai, M., 2022. Transport of black carbon from central and west Asia to the Tibetan plateau: seasonality and climate effect. Atmos. Res. 267, 105987.
Huang, Y., Lu, X., Fung, J.C.H., Wong, D.C., Li, Z., Chen, Y., Chen, W., 2023. Investigating Southeast Asian biomass burning by the WRF-CMAQ two-way coupled model: emission and direct aerosol radiative effects. Atmos. Environ. 294, 119521.
Lee, H.-M., Park, R., Henze, D., Lee, S., Shim, C., Shin, H.-J., Moon, K., Woo, J.-H., 2017. PM2:5 source attribution for Seoul in May from 2009 to 2013 using GEOS-Chem and its adjoint model. Environ. Pollut. 221, 377–384.
Li, W., Wang, Y., Yi, Z., Guo, B., Chen, W., Che, H., Zhang, X., 2024a. Evaluation of MERRA-2 and CAMS reanalysis for black carbon aerosol in China. Environ. Pollut. 34, 123182.
Li, Y., Kang, S., Chen, J., Hu, Z., Wang, K., Paudyal, R., Liu, J., Wang, X., Qin, X., Sillanpää, M., 2019. Black carbon in a glacier and snow cover on the northeastern Tibetan Plateau: concentrations, radiative forcing and potential source from local topsoil. Sci. Total Environ. 686, 1030–1038.
Li, K., Liao, H., Mao, Y.-H., Ridley, D.A., 2016. Sectoral and regional contributions to black carbon and its direct radiative forcing in China. Atmos. Environ. 124, 351–366.
Li, K., Wang, X., Lu, X., Chen, H., Yang, X., 2021. Effect of pollution level on size distributions and mixing state of ambient black carbon particles in an urban area during wintertime. Aerosol Air Qual. Res. 21, 9.
Li, X., Zhou, J., Wang, J., Feng, Z., 2023. Study on spatial changes in PM2.5 before and after the COVID-19 pandemic in southwest China. Atmosphere 14, 671.
Li, J., Fan, W., Wu, J., Han, Z., Li, J., Zhang, C., Liang, L., 2024b. Impacts of open biomass burning in Southeast Asia on atmospheric $PM_{2.5}$ concentrations over south China from 2009 to 2018. Atmos. Environ. 327, 120491.
Li, J., Han, Z., Surapipith, V., Fan, W., Thongboonchoo, N., Wu, J., Li, J., Tao, J., Wu, Y., Macatangay, R., Bran, S., Yu, E., Zhang, A., 2022. Direct and indirect effects and feedbacks of biomass burning aerosols over Mainland Southeast Asia and South China in springtime. Sci. Total Environ. 842, 156949.
Lian, P., Zhao, K., Yuan, Z., 2024. AIRS and MODIS satellite-based assessment of air pollution in southwestern China: impact of stratospheric intrusions and cross-border transport of biomass burning. Remote Sens. 16, 2409.
Lin, J., Han, D., Chen, F., Zhang, X., Yang, Y., Yang, L., Gui, H., Yu, Z., Cao, L., Shi, J., Jiang, G., 2025. Atmospheric black carbon (BC) in Hangzhou, China: temporal variation, source apportionment, and case study of the 19th Asian Games. Environ. Pollut. 369, 125852.
Lin, W., Dai, J., Liu, R., Zhai, Y., Yue, D., Hu, Q., 2019. Integrated assessment of health risk and climate effects of black carbon in the Pearl River Delta region, China. Environ. Res. 176, 108522.
Lin, C.-Y., Hsu, H.-M., Lee, Y.H., Kuo, C.H., Sheng, Y.-F., Chu, D.A., 2009. A new transport mechanism of biomass burning from Indochina as identified by modeling studies. Atmos. Chem. Phys. 9, 7901–7911.
Lin, S.-J., Rood, R.B., 1996. Multidimensional flux-form semi-Lagrangian transport schemes. Mon. Weather Rev. 124, 2046–2070.
Liu, X., Wang, S., Zhang, Q., Jiang, C., Liang, L., Tang, S., Zhang, X., Han, X., Zhu, L., 2023. Origins of black carbon from anthropogenic emissions and open biomass burning transported to Xishuangbanna, Southwest China. J. Environ. Sci. 125, 277–289.
Liu, Y., Chen, J., Shi, Y., Zheng, W., Shan, T., Wang, G., 2024. Global emissions inventory from open biomass burning (GEIOBB): utilizing fengyun-3D global fire spot monitoring data. Earth Syst. Sci. Data 16, 3495–3515.
Lu, M., Zheng, J., Huang, Z., 2021. Insight into the characteristics of carbonaceous aerosols at urban and regional sites in the downwind area of Pearl River Delta region. China. Sci. Total Environ. 778, 146251.
Ma, J., Xu, J., Qu, Y., 2020. Evaluation on the surface $PM_{2.5}$ concentration over China mainland from NASA's MERRA-2. Atmos. Environ. 237, 117666.
Mao, M., Zhou, Y., Zhang, X., 2023. Evaluation of MERRA-2 black carbon characteristics and potential sources over China. Atmosphere 14, 1378.
Mao, Y.-H., Liao, H., Han, Y., Cao, J., 2016. Impacts of meteorological parameters and emissions on decadal and interannual variations of black carbon in China for 1980–2010. J. Geophys. Res. Atmos. 121, 1822–1843.
Mao, Y.-H., Zhao, X., Liao, H., Zhao, D., Tian, P., Henze, D., Cao, H., Zhang, L., Li, J., Li, J., Ran, L., Zhang, Q., 2020. Sources of black carbon during severe haze events in the Beijing–Tianjin–Hebei region using the adjoint method. Sci. Total Environ. 740, 140149.
Mao, Y.-H., Shang, Y., Liao, H., Cao, H., Qu, Z., Henze, D., 2024. Sensitivities of ozone to its precursors during heavy ozone pollution events in the Yangtze River Delta using the adjoint method. Sci. Total Environ. 925, 171585.
Menegoz, M., Voldoire, A., Teyssedre, H., Alasyelia, D., Peuch, V.-H., Gouttevin, I., 2011. How does the atmospheric variability drive the aerosol residence time in the Arctic region? Tellus B 64, 11596.
Miao, H., Dong, D., Haung, G., 2020. Evaluation of Northern Hemisphere surface wind speed and wind power density in multiple reanalysis datasets. Energy 20, 117382.
McDuffie, E., Smith, S., O'Rourke, P., Tibrewal, K., Venkataraman, C., Marais, E., Zheng, B., Crippa, M., Brauer, M., Martin, R., 2020. A global anthropogenic emission inventory of atmospheric pollutants from sector- and fuel-specific sources (1970–2017): an application of the Community Emissions Data System. CEDS) 12, 3413–3442.
Nam, J.J., Gustafsson, O., Kurt-Karakus, P., Breivik, K., Steinnes, E., Jones, K., 2008. Relationships between organic matter, black carbon and persistent organic pollutants in European background soils: implications for sources and environmental fate. Environ. Pollut. 156, 809–817.
Pang, N., Jiang, B., Zheng, Y., 2023. The impact of fireworks burning on air quality and their health effects in China during Spring Festivals of 2015–2022. Atmos. Pollut. Res. 14, 101888.
Park, R.J., Jacob, D.J., 2003. Sources of carbonaceous aerosols over the United States and implications for natural visibility. J. Geophys. Res. 108 (D12), 4355.
Park, R.J., Jacob, D.J., Palmer, P.I., 2005. Export efficiency of black carbon aerosol in continental outflow: global implications. J. Geophys. Res. 110, D11205.
Pauraite, J., Mainelis, G., Kecorius, S., Minderyte, A., Dudoitis, V., Garbariene, I., PlauSkaitE, K., Ovadnevaite, J., BycenkienE, S., 2021. Office indoor pm and bc level in Lithuania: the role of a long-range smoke transport event. Atmosphere 10, 1047.
Pei, C., Wu, Y., Tao, J., Zhang, L., Zhang, T., Zhang, R., Li, S., 2023. Seasonal variations of mass absorption efficiency of elemental carbon in $PM_{2.5}$ in urban Guangzhou of South China. J. Environ. Sci. 133, 83–92.
Qi, L., Li, Q., Henze, D., Tseng, H., He, C., 2017. Sources of springtime surface black carbon in the Arctic: an adjoint analysis for April 2008. Atmos. Chem. Phys. 17, 9697–9716.
Qin, W., Zhang, Y., Chen, J., Yu, Q., Cheng, S., Li, W., Liu, X., Tian, H., 2019. Variation, sources and historical trend of black carbon in Beijing, China based on ground observation and MERRA-2 reanalysis data. Environ. Pollut. 245, 853–863.
Randerson, J.T., van der Werf, G.R., Giglio, L., Collatz, G.J., Kasibhatla, P.S., 2017. Global fire emissions Database, version 4.1 (GFEDv4). 2017. Global fire emissions estimates during 1997–2016. Earth Syst. Sci. Data 9, 697–720.

Rasking, L., Koshy, P., Bongaerts, E., Bove, H., Amelot, M., Plusquin, M., Vusser, K., Nawrot, T., 2023. Ambient black carbon reaches the kidneys. Environ. Int. 177, 107997.
Roy, D., Lim, H., Kim, S., Song, S., Park, J., 2024. Particulate matter and black carbon exposure in Seoul subway: implications for human health risk. J. Build. Eng. 95, 110091.
Walcek, C.J., Brost, R.A., Chang, J.S., 1986. SO_2, sulfate and HNO_3 deposition velocities computed using regional landuse and meteorological data. Atmos. Environ. 20 (5), 949–964.
Wang, J., Heever, S.C., Reid, J.S., 2009. A conceptual model for the link between Central American biomass burning aerosols and severe weather over the south central United States. Environ. Res. Lett. 4, 015003.
Wei, M., Chuai, X., Li, Y., Han, J., Zhang, C., 2024. Decoupling analysis between socio-economic growth and air pollution in key regions of China. Sustainability 16, 7571.
Wu, L., Su, H., Zeng, X., Posselt, D., Wong, S., Chen, S., Stoffelen, A., 2024. Uncertainty of atmospheric winds in three widely used global reanalysis datasets. J. Clim. Appl. Meteorol. 63, 166–180.
Xu, J., Martin, R.V., Morrow, A., Sharma, S., Huang, L., Leaitch, W.R., Burkart, J., Schulz, H., Zanatta, M., Willis, M.D., Henze, D.K., Lee, C.J., Herber, A.B., Abbatt, J.P. D., 2017. Source attribution of Arctic black carbon constrained by aircraft and surface measurements. Atmos. Chem. Phys. 17, 11971–11989.
Xu, X., Yang, X., Zhu, B., Tang, Z., Wu, H., Xie, L., 2020. Characteristics of MERRA-2 black carbon variation in east China during 2000–2016. Atmos. Environ. 222, 117140.
Yang, J., Mao, F., Zang, L., Zhang, Y., Hong, J., Yin, J., Chen, J., 2022a. Why do extreme particulate pollution events occur in low-emission Yunnan Province, China? Atmos. Environ. 289, 119336.
Yang, L., Mao, Y.-H., Liao, H., Xie, M., Zhang, Y., 2024. Direct radiative forcing of light-absorbing carbonaceous aerosols in China. Atmos. Res. 304, 107396.
Yang, Q., Zhao, T., Tian, Z., 2022b. The cross-border transport of $PM_{2.5}$ from the southeast asian biomass burning emissions and its impact on air pollution in Yunnan plateau, southwest China. Remote Sens. 14, 1886.
Yang, S., Lau, W.K.M., Ji, Z., Dong, W., Yang, S., 2022c. Impacts of radiative effect of pre-monsoon biomass burning aerosols on atmospheric circulation and rainfall over Southeast Asia and southern China. Clim. Dyn. 59, 417–432.
Yang, Y., Wang, H., Smith, J.S., Ma, P.-L., Rasch, J.P., 2017. Source attribution of black carbon and its direct radiative forcing in China. Atmos. Chem. Phys. 17, 4319–4336.
Yin, S., Wang, X., Zhang, X., et al., 2019. Influence of biomass burning on local air pollution in mainland Southeast Asia from 2001 to 2016. Environ. Pollut. 254, 112949.
Yin, S., 2020. Biomass burning spatiotemporal variations over South and Southeast Asia. Environ. Int. 145, 106153.
Zhang, B., Lindzen, R.S., Tallapragada, V., Weng, F., Liu, Q., Sippel, J., Ma, Z., Bender, M., 2016a. Increasing vertical resolution in US models to improve track forecasts of Hurricane Joaquin with HWRF as an example. PANS 113, 11765–11769.
Zhang, G., McFarlane, N.A., 1995. Sensitivity of climate simulations to the parameterization of cumulus convection in the Canadian Climate Centre general circulation model. Atmos.-Ocean 33 (3), 407–446.
Zhang, G., Wang, M., Yang, B., Liu, K., 2024. Current and future patterns of global wildfire based on deep neural networks. Earths Future 12, e2023EF004088.
Zhang, L., Liu, L., Zhao, Y., Gong, S., Zhang, X., Henze, D., Capps, S., Fu, T., Zhang, Q., Wang, Y., 2015. Source attribution of particulate matter pollution over North China with the adjoint method. Environ. Res. Lett. 10, 084011.
Zhang, L., Ding, S., Qian, W., Zhao, A., Zhao, S., Yang, Y., Weng, G., Tao, M., Chen, H., Zhao, S., Wang, Z., 2022. The Impact of long-range transport of biomass burning emissions in Southeast Asia on Southern China. Atmosphere 13, 1029.
Zhang, Q., Shen, Z., Ning, Z., Wang, Q., Cao, J., Lei, Y., Sun, J., Zeng, Y., Westerdahl, D., Wang, X., Wang, L., Xu, H., 2018. Characteristics and source apportionment of winter black carbon aerosols in two Chinese megacities of Xi'an and Hong Kong. Environ. Sci. Pollut. Res. 25, 33783–33793.
Zhang, Y., Yang, Y., Li, J., Wang, Y., Wang, Z., 2016b. Modeling the impacts of biomass burning in southeast Asia on $PM_{2.5}$ over China in spring. Res. Environ. Sci. 29, 952–962.
Zhang, Z., Zhou, L., Zhang, M., 2025. A numerical sensitivity study on the snow-darkening effect by black carbon deposition over the Arctic in spring. Atmos. Chem. Phys. 25, 1–25.
Zheng, B., Tong, D., Li, M., Liu, F., Hong, C., Geng, G., Li, H., Li, X., Peng, L., Qi, J., Yan, L., Zhang, Y., Zhao, H., Zheng, Y., He, K., Zhang, Q., 2018. Trends in China's anthropogenic emissions since 2010 as the consequence of clean air actions. Atmos. Chem. Phys. 18, 14095–14111.
Zhou, Y., Ma, X., Tian, R., Wang, K., 2023. Seasonal transition of black carbon aerosols over Qinghai-Tibet Plateau: simulations with WRF-Chem. Atmos. Environ. 308, 119866.
Zhou, Y., Yang, J., Kang, S., Hu, Y., Chen, X., Xu, M., Ma, M., 2024. Weakened black carbon trans-boundary transport to the Tibetan Plateau during the COVID-19 pandemic. Sci. Total Environ. 916, 170208.
Zhu, C., Zhou, X., Zhao, P., Chen, L., He, J., 2011. Onset of East Asian subtropical summer monsoon and rainy season in China. Sci. China Earth Sci. 54, 1845–1853.
Zhu, J., Yue, X., Zhou, H., Che, H., Xia, X., Wang, J., Zhao, T., Tian, C., Liao, H., 2024. The multi-year contribution of Indo-China peninsula fire emissions to aerosol radiation forcing in southern China during 2013–2019. Sci. Total Environ. 927, 172337.
Zhuang, B., Zhou, Y., Hu, Y., Liang, S., Gao, P., Gao, Y., Chen, H., Li, S., Wang, T., Xie, M., Li, M., 2025. Influence of ship emitted sulfur and carbonaceous aerosols on East Asian climate in summer. Atmos. Environ. 344, 121035.
Zong, Y., Xiao, Q., Lu, S., 2016. Black carbon (BC) of urban topsoil of steel industrial city (Anshan), Northeastern China: concentration, source identification and environmental implication. Sci. Total Environ. 569–570, 990–996.